CHAPTER
7
Strike-Slip Faults

Strike-slip faults are generally vertical faults that accommodate horizontal shear within the crust. Their traces on the Earth's surface may vary from straight to gently curved (Figure 7.1). Displacement on a given fault may be either right-lateral or left-lateral, and it results in no net addition or subtraction of area to the crust. In some cases, oblique strike-slip motion results from the addition of a component of horizontal contraction or extension perpendicular to the fault trace. Strike-slip faults exist on all scales in both oceanic and continental crust. In this chapter we concentrate on the geologic structures associated with continental strike-slip faults.

Tear faults are relatively small-scale, local strike-slip faults that are commonly subsidiary to other structures such as folds, thrust faults, or normal faults (see, for example, Figures 6.7*C*, *D* and 6.13). They are steeply dipping and oriented subparallel to the regional direction of displacement. They occur in the hanging wall blocks of low-angle faults and accommodate different amounts of displacement either on different parts of the fault or between the allochthon and adjacent autochthonous rocks.

The term transfer fault is applied to two different geometries of strike-slip faults. In extensional terranes they are parallel to the regional direction of displacement and mark domains of different normal fault geometry and displacement (see Figures 5.11, 5.12). Imbricate systems of normal faults—and possibly their detachments—terminate against such transfer faults and may have different amounts of displacement and different orientations from the normal faults in adjacent domains. There is no clear distinction between these faults and the tear faults described above, except perhaps that transfer faults may be of larger scale and may accommodate larger amounts of slip. In strike-slip terranes, transfer faults lie at a high angle to the regional direction of displacement and connect adjacent or *en echelon* parallel strike-slip faults. They accommodate the transfer of displacement from one fault to the next, and slip on these faults is generally oblique.

Transform faults and transcurrent faults are major regional strike-slip fault systems that generally comprise zones of many associated faults (Figure 7.2). Transform faults are strike-slip faults that form segments of lithospheric plate boundaries (Figure 7.2*A*). Transcurrent faults, on the other hand, are regional-scale strike-slip faults in continental crust that are not parts of plate margins[1] (Figure 7.2*B*). Both types of faults may be many hundreds of kilometers long and may have accumulated relative displacements of up to several hundred kilometers.

---

[1] The specific usage of these two terms is not universally agreed on. The confusion arises in part from the fact that before the development of plate tectonics, *transcurrent fault* was used to refer to all major strike-slip faults, some of which are now recognized to be plate boundaries. Moreover, *transform fault* originally referred to faults connecting offset segments of oceanic spreading ridges. Its use has now been generalized to include all plate boundary strike-slip faults. *Wrench fault* is another term used to refer to strike-slip faults in a variety of specific senses. (We do not use this term.)

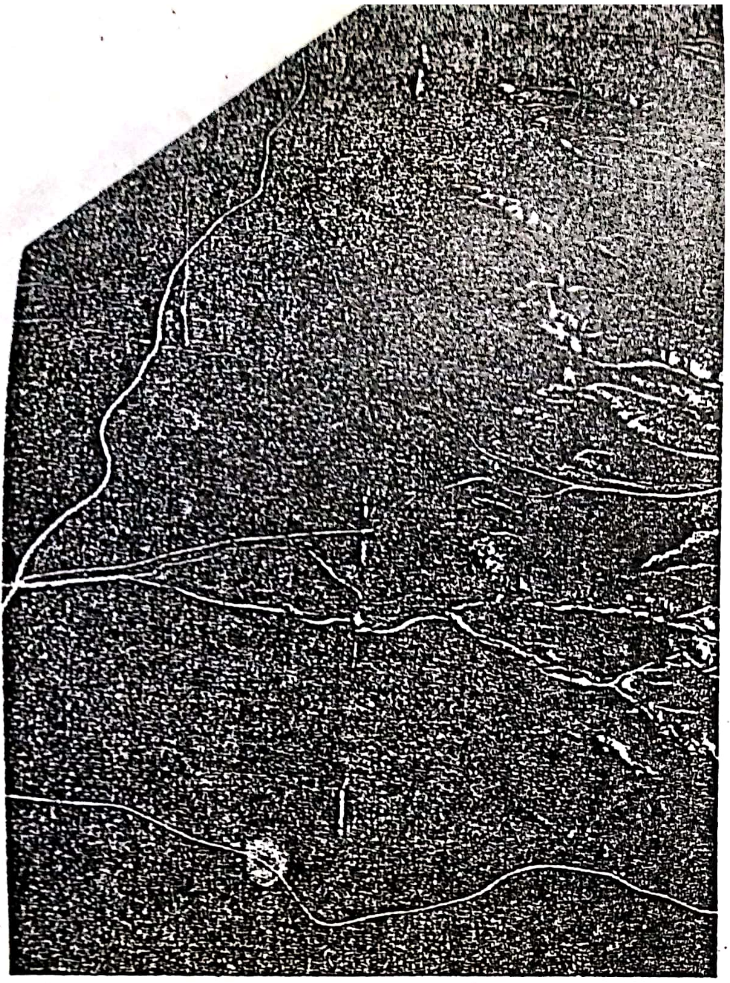

A.

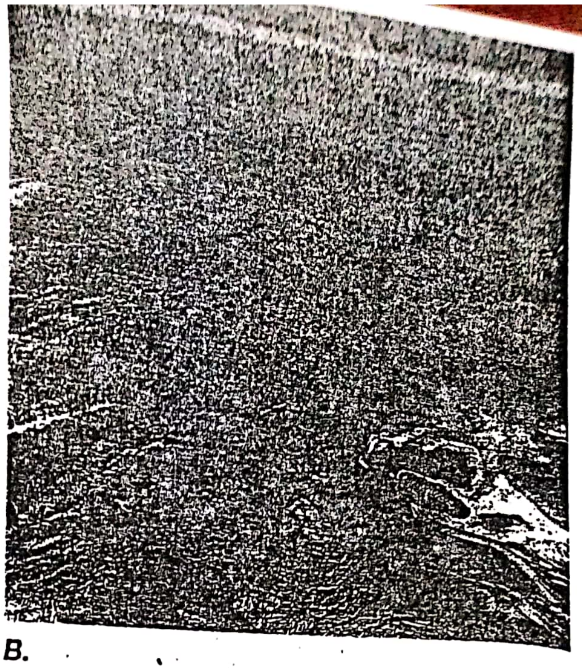

B.

Figure 7.1 Photographs of strike-slip faults illustrating rectilinear fault traces. *A.* San Andreas fault, Carrizo plain, California. Aerial view looking northwest along trace of the San Andreas fault. *B.* Landsat image of Altyn Tagh fault, China showing through-going nature of the structure (see location in Figure 7.2*B*).

At outcrop or local scale, transform and transcurrent faults are indistinguishable. One must identify them on the basis of the regional plate tectonic environment and the tectonic role that each plays. For most plates, recognizing a transform boundary is straightforward. In a few situations, however, such as in Asia (Figure 7.2*B*), the distinction between transform and transcurrent faults depends in part on how small a block one chooses to accept as a "tectonic plate."

The San Andreas fault system of California (Figures 7.1*A* and 7.2*A*), is a right-lateral transform fault system 1300 km long that connects two triple junctions, one south of the Gulf of California and the other at Cape Mendocino on the north coast of California. It consists of many roughly parallel faults in a zone as much as 100 to 150 km wide. It displays along its length many of the characteristic features of strike-slip faults, and because it has been exceptionally well studied, it furnishes numerous examples of structures that we describe in the following sections.

Central and eastern Asia contains a complex system of transcurrent faults (Figures 7.1*B* and 7.2*B*), dominated by left-lateral faults in eastern Tibet and by right-lateral faults in an area extending from Lake Baikal in the northeast to the Quetta-Chaman fault in the southwest. Many workers attribute this complex system of faults to the effects of the northward-moving Indian plate impinging against the Asian crustal block, and this model accounts for many of the observed features. Several examples of characteristic strike-slip fault structures that we discuss in the following sections come from this complex.

7.1 Characteristics of Strike-Slip Faults

Most strike-slip faults are approximately planar and vertical, at least near the surface of the Earth. As a result, their fault traces tend to be straight lines on a map, even across rugged topography. Many large strike-slip faults are marked by prominent continuous topographic features on the Earth's surface that are visible even from space (Figure 7.1*B*). The topographically high side of a strike-slip fault commonly changes from one side to the other along the fault trace. The topographic

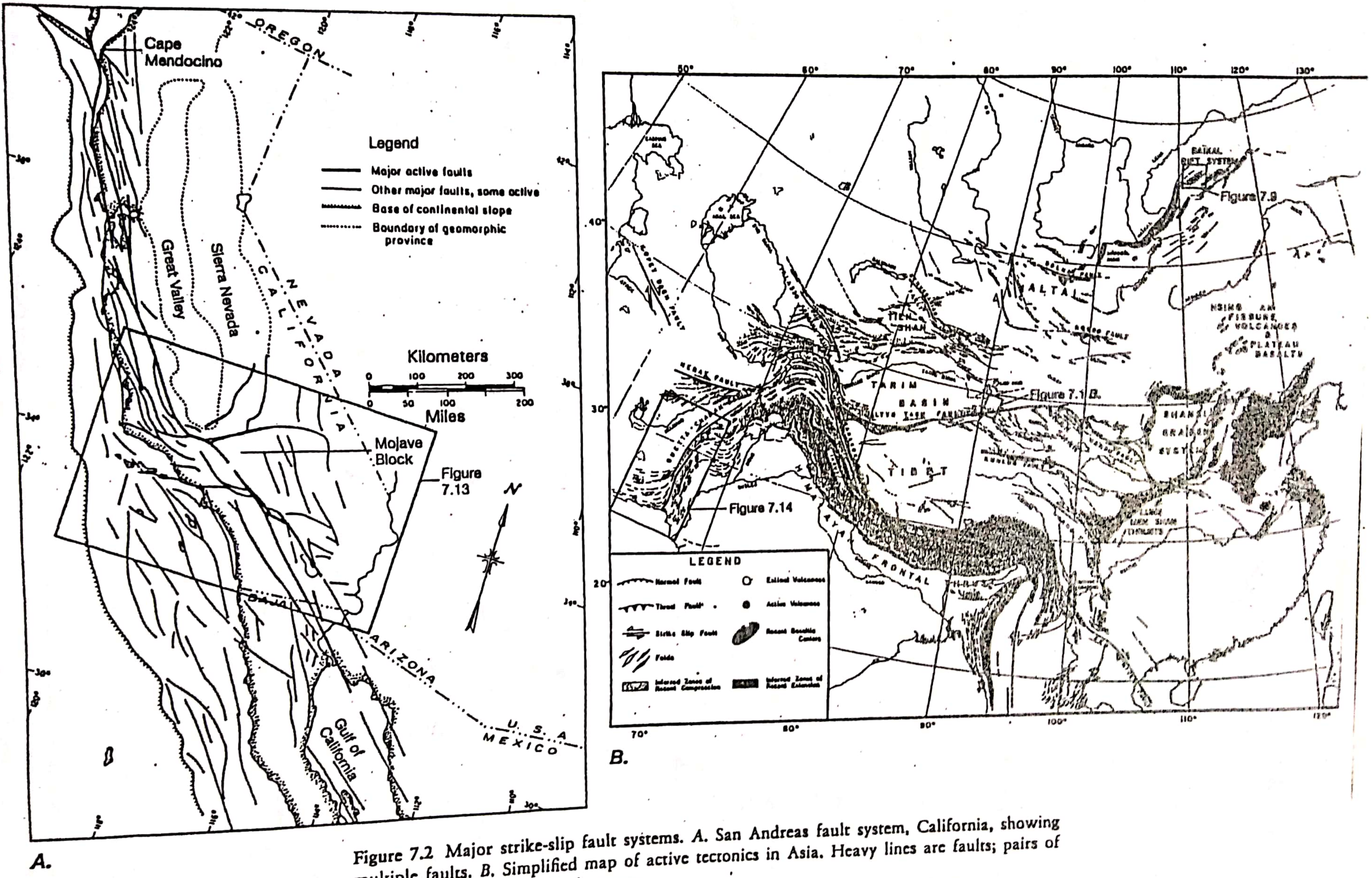

Figure 7.2 Major strike-slip fault systems. *A.* San Andreas fault system, California, showing multiple faults. *B.* Simplified map of active tectonics in Asia. Heavy lines are faults; pairs of arrows indicate sense of displacement.

expression of the fault may result from minor components of vertical slip along segments of the fault associated with a component of contraction or extension across the fault, with differences in temperature of the rocks across the fault, with juxtaposition of originally separated topographic features, or with juxtaposition of rocks that differ in resistance to erosion.

The dominantly horizontal slip on strike-slip faults produces a horizontal separation that often is used as an indication of strike-slip faulting. If the cutoff line of the bedding on the fault is parallel to the displacement, however, no separation is evident (Figure 7.3*A*). If beds are inclined such that their cutoff lines are oblique to the displacement, the separation on a vertical cross section of the fault can be either right-side-up (Figure 7.3*B*) or left-side-up (Figure 7.3*C*), depending on the relative orientation of the beds and the fault and on the sense of displacement on the fault. Large strike separations of a planar boundary, such as a lithologic contact, amounting to many tens or hundreds of kilometers constitute reasonable evidence for strike-slip faulting (see Figure 4.18), although small strike separations can result from other types of fault slip (see Figures 5.2 and 6.2).

Strike-slip faults display the typical features that we discussed in Chapter 4. Slickenside lineations are subhorizontal. Drag folds may form along some strike-slip faults if the bedding is favorably oriented (Section 4.2), although folds reflecting distributed deformation on either side of the fault are more common (see Figure 7.4*B* and the following discussion). Geomorphic features characteristic of strike-slip faults include linear erosional depressions (Figure 7.1*A*), sag ponds, springs, and offset streams (Figure 4.13) and topography, including shutter ridges, which occur where ridge and canyon topography is transected by a strike-slip fault, and a segment of a ridge has been displaced in front of a canyon, shutting it off.

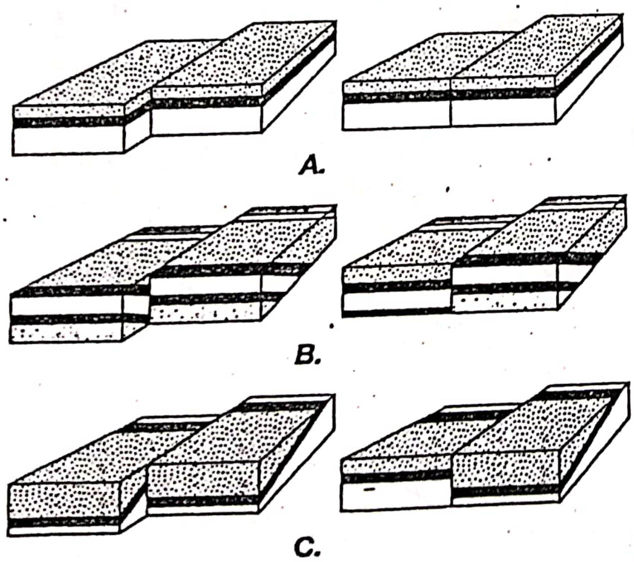

Figure 7.3 Separations of stratigraphic units as a result of left-lateral (sinistral) strike-slip faulting. Drawings on the right show vertical sections after faulting.

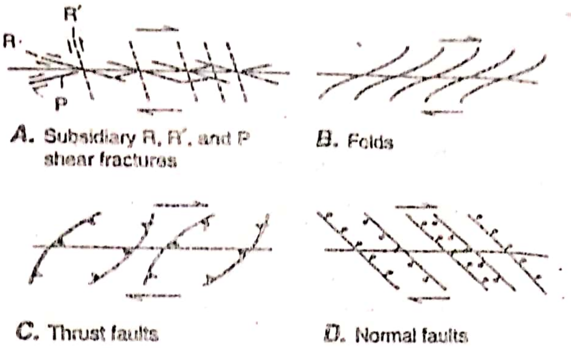

A. Subsidiary R, R', and P shear fractures

B. Folds

C. Thrust faults

D. Normal faults

Figure 7.4 Structures associated with strike-slip faults and their orientations relative to the shear sense on the fault.

A variety of shear fractures, folds, normal faults, and thrust faults are found associated with strike-slip faults. The orientations of these structures relative to the main strike-slip fault are characteristic of the sense of shear on the fault (Figure 7.4). Subsidiary shear fractures, known as Riedel shears or R shears, develop at a small angle (roughly 10° to 20°) to the main fault in an *en echelon* array (Figure 7.4*A*). R shears are synthetic to the main fault, which means they are subparallel and have the same shear sense, and the acute angle formed by the traces of the R shear and the main fault points in the direction of relative motion of the block containing the R shear. Other subsidiary shears may also develop. P shears are synthetic to the main fault and are oriented symmetrically with respect to the fault from the orientation of the R shears. Conjugate Riedel shears, or R′ shears, are antithetic shear fractures that are oriented at high angles to the fault (roughly 70° to 80°) and have a shear sense opposite to that of the main fault. On a small scale, these various secondary shear fractures are responsible for some of the sense-of-shear criteria for brittle faulting that we discuss in Section 4.3 (see Figure 4.16). On a large scale, they can form a complex anastomosing network of faults that become very difficult to interpret.

Folds and thrust faults form in an *en echelon* arrangement above or beside major strike-slip faults (Figure 7.4*B, C*). The trend of the fold hinges and the strike of the thrust faults are oriented at 45° or less to the strike-slip fault, and the acute angle defined by the intersection of the strike-slip fault trace with the fold hinge or the thrust fault trace points in the direction of relative motion of the fault block *opposite* the one containing the fold or thrust. These structures record a component of contraction oblique to the strike-slip fault and

---

roughly perpe
thrust faults.
Normal
along strike-sl
45° to the ma
orientations
faults (Figure
the intersecti
mal faults po
the block cor
record a com
strike-slip fa
faults and th
and thrust f
Many
result of the
the displace
7.2. Other s
displacemen
in Section 7

7.2 Sh
St

Single Fa

At depth,
fault, suc
continue

roughly perpendicular to the trends of the folds and the thrust faults.

Normal faults may also form *en echelon* arrays along strike-slip faults, and they are oriented at roughly 45° to the main fault and close to perpendicular to the orientations characteristic of fold hinges and thrust faults (Figure 7.4*D*). Thus the acute angle defined by the intersection of the traces of the strike-slip and normal faults points in the direction of relative motion of the block containing the normal fault. These structures record a component of extension that is oblique to the strike-slip fault and is perpendicular to both the normal faults and the contraction orientation recorded by folds and thrust faults.

Many of these associated structures develop as a result of the inherent geometry of strike-slip faults and the displacement along them, as we discuss in Section 7.2. Other structures reflect a distributed component of displacement along or across the fault, as we describe in Section 7.4.

7.2 Shape, Displacement, and Related Structures

Single Faults

At depth, strike-slip faults may terminate on another fault, such as a low-angle detachment, or they may continue through the crust and lose their identity at depth in a zone of ductile deform
along modern strike-slip faults typical
down to depths of about 15 km. Bel
zone, aseismic shear is probably accomm
taclastic deformation in a transition zone—
that by ductile deformation. A strike-slip fa
nating against a horizontal detachment is geome
equivalent to a dip-slip fault terminating against a
tical tear fault.

Although they are characteristically vertical with straight map traces, strike-slip faults also include bends (or jogs) and stepovers (or offsets) (Figure 7.5). Bends are curved parts of a continuous fault trace that connect two noncoplanar segments of fault. Stepovers are regions where one fault ends and another *en echelon* fault of the same orientation begins. Bends and stepovers are described geometrically as being either right or left depending on whether the bend or step is to the right or to the left as one progresses along the fault. This description remains the same regardless of the sense of shear on the fault zone. Bends are geometrically equivalent to frontal ramps on dip-slip faults.

Displacement on strike-slip faults ideally is horizontal and therefore parallel to the strike of the fault. For a vertical fault, the trace of the fault on any topographic surface is straight and parallel to strike—and therefore also parallel to the ideal displacement direction. We describe a bend or stepover kinematically as contractional or restraining, if material is pushed together by the dominant fault shear (dashed arrow pairs, Figure 7.5*A*, *D*); the bend or stepover is extensional,

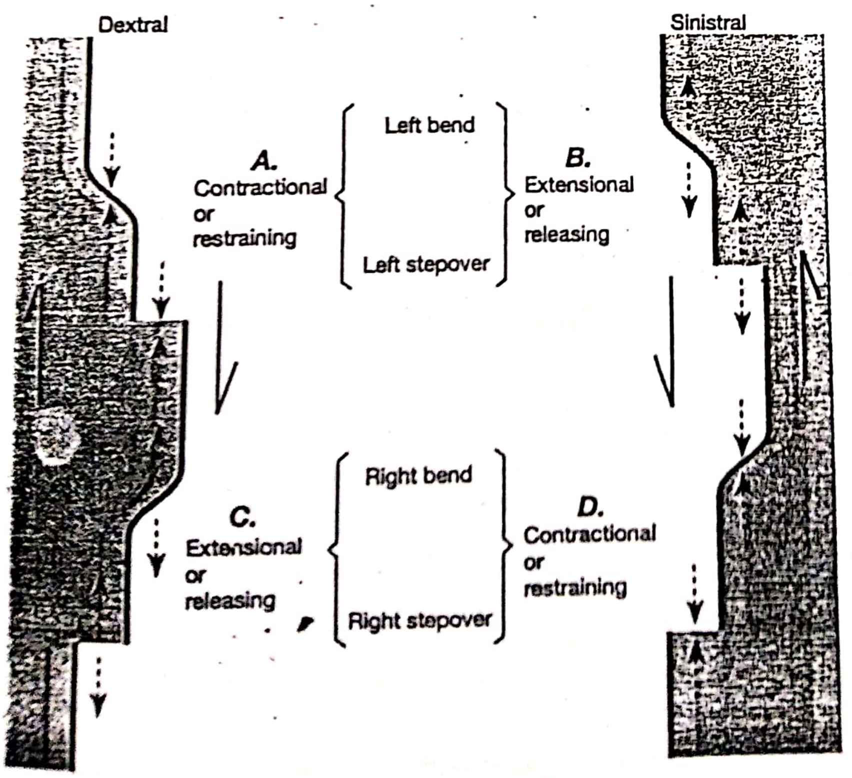

Figure 7.5 The geometry and terminology for right and left bends and stepovers. Large arrows show relative shear on the fault. Pairs of dashed arrows indicate the extension or contraction across the bends and stepovers.

w pairs, Figure 7.5B, C). 7.5A, C), right bends and and left bends and stepovers whereas on sinistral faults (Figure s and stepovers are extensional and stepovers are contractional. Thus bends, and broad curves in the trace of a strike-slip not permit pure strike-slip motion but require accommodating deformation.

Strike-Slip Duplexes

Displacement along strike-slip faults with bends or stepovers produces a complex zone of deformation. Commonly the result is a strike-slip duplex, which is a set of horizontally stacked horses bounded on both sides by segments of the main fault (see Figure 4.26C). Such a duplex may be extensional (Figure 7.6) or contractional (Figure 7.7), depending on whether it forms at an extensional or a contractional bend or stepover.

Strike-slip duplexes must differ from duplexes that form along dip-slip faults, because the different orientation of the shear plane places different constraints on the deformation. For dip-slip faults, the faulting accommodates either a thickening or a thinning of the crust, which results in a vertical displacement of the surface of the Earth, which is a free surface (Figure 4.26A, B). For strike-slip faults, however, the corresponding thick direction (Figure 4.26C), which is impossible because of the constraint imposed by the rest of the crust. There being no free vertical surface, the required thickening or thinning can be accommodated only by vertical motion of the free horizontal surface, and therefore slip on strike-slip duplex faults cannot be purely strike-slip but must be oblique. To accommodate this component of motion, faults in a strike-slip duplex must have a different geometry from those in dip-slip duplexes.

The oblique slip on the faults bounding the horses in an extensional strike-slip duplex must be a combination of strike-slip and normal slip (Figure 7.6C); on the faults in a contractional strike-slip duplex, it must be a combination of strike-slip and reverse slip (Figure 7.7C). The shortening associated with contractional duplexes can also be accommodated by folding subparallel to the reverse faults (see Figure 7.4). The deformation required at contractional or extensional bends provides one mechanism for producing the *en echelon* folds and the normal faults and thrust faults associated with strike-slip faults that we describe in Section 7.1 (Figure 7.4; see also Figure 7.13).

In a strike-slip duplex, the shape of the faults on the vertical section normal to the main fault trace is referred to as a flower structure. If the dip-slip component is normal, the faults tend to be concave up and to form a normal, or negative, flower structure, also known as tulip structure (Figures 7.6C, 7.8A). If the dip-slip component is reverse, the faults tend to be con-

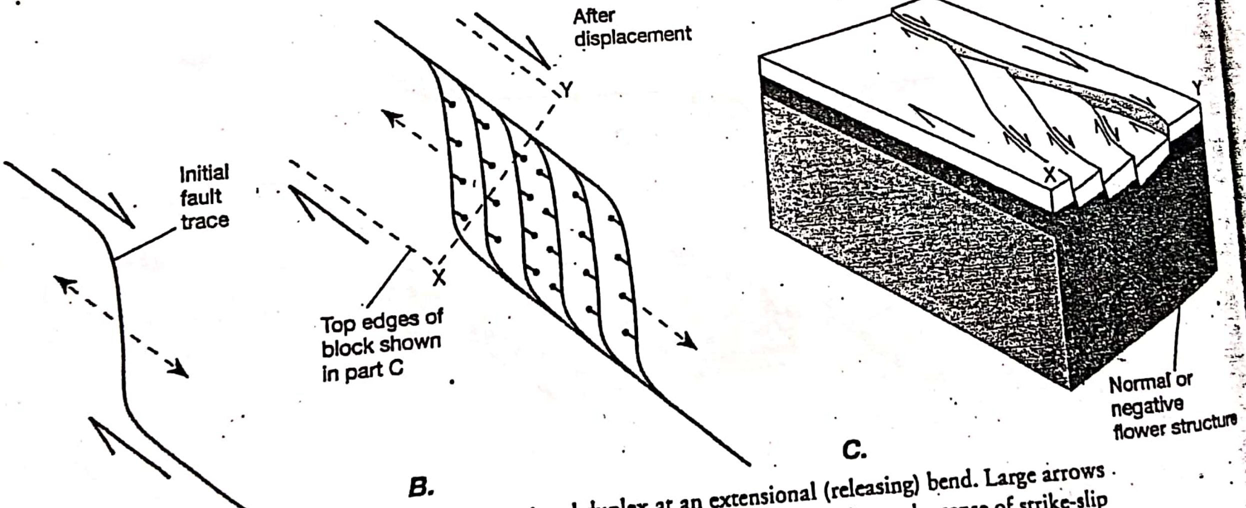

Figure 7.6. Formation of an extensional duplex at an extensional (releasing) bend. Large arrows indicate the dominant shear sense of the fault zone; small arrows indicate the sense of strike-slip and normal components of motion on the fault splays. *A.* Extensional bend on a dextral strike-slip fault. *B.* An extensional duplex developed from the bend in part *A*. *C.* A block diagram showing a normal, negative, flower structure in three dimensions. The block faces are vertical planes along the dashed lines in part *B*.

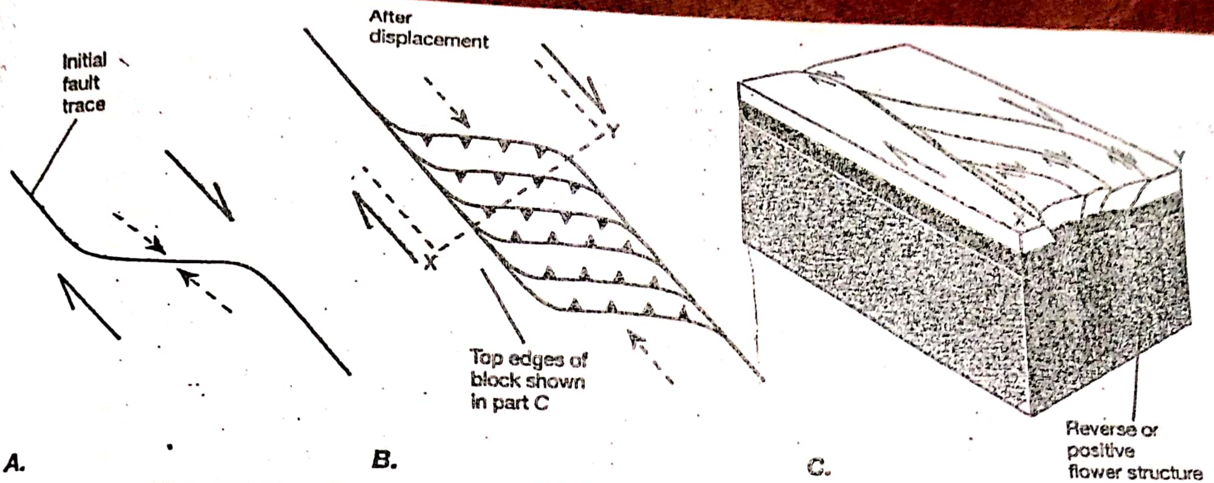

Figure 7.7 Formation of a contractional duplex at a contractional (restraining) jog. Large arrows indicate the dominant shear sense of the fault zone; small arrows indicate the sense of strike-slip and reverse components of motion on the fault splays. *A.* Contractional bend on a dextral fault. *B.* A contractional duplex developed from the bend in part *A.* *C.* A block diagram showing reverse, or positive, flower structure in three dimensions. The block faces are vertical planes along the dashed lines in part *B.*

vex up and to form a reverse, or positive, flower structure, also known as palm tree structure (Figures 7.7C, 7.8B). All these botanical names suggest the similarity in cross-sectional form between the plants and the faults, but given the difference in the third dimension, they are not particularly apt.

In actual cases, the slip on faults in strike-slip duplexes may vary along strike from having a normal component at one end to having a thrust component at the other. Such faults, which are sometimes called scissor faults, accommodate the rotation of horst blocks in the duplex.

Examples of these two types of flower structures can be seen in seismic reflection profiles from the southern Andaman Sea (Figure 7.8*A*) and from the Ardmore Basin in southern Oklahoma (Figure 7.8*B*). In Figure 7.8*A*, the grabenlike offset of reflectors across the upper faults in the fault zone indicates a component of normal slip that is characteristic of normal (negative) flower structure. In Figure 7.8*B*, the major faults show a component of thrusting that is characteristic of reverse (positive) flower structure.

Displacement at extensional bends and stepovers produces topographic depressions known as pull-apart basins, which commonly fill with water to produce sag ponds or lakes. On a large scale, pull-apart basins are usually rhomb-shaped, fault-bounded basins several kilometers or tens of kilometers in dimension (Figure 7.9). Faulting may be accompanied by volcanic eruptions that cover the floor of the basin. Because they form topographic depressions, pull-apart basins generally accumulate large thicknesses of alluvial and/or lake deposits. With continued displacement, the basin may eventually be split by a younger segment of the fault, which separates opposite sides of the basin from each other.

Terminations

Strike-slip faults can terminate in the crust at a zone of either extensional or contractional deformation, depending on the location of the deformation zone relative to the slip vectors on the fault. Extension may be accommodated where strike-slip faults splay and turn into an imbricate fan of normal faults (Figure 7.10*A*, *B*). Similarly, contraction may be accommodated by an imbricate fan of thrust faults and/or folds (Figure 7.10*C*, *D*). Within such zones, strike-slip displacement diminishes progressively to zero along the fault.

In some cases, the fault may branch into a fan of strike-slip splay faults (also called a horsetail splay) that commonly curve toward the receding fault block (Figure 7.10*E*). The displacement on any individual splay is relatively small, but the sum of the displacements on all the faults in the splay equals the displacement on the main strike-slip fault. The fan thereby distributes the deformation through a large volume of crust. The geometry of a horsetail splay on a strike-slip fault is comparable to that of an imbricate fan of listric faults on a low-angle thrust fault or normal fault.

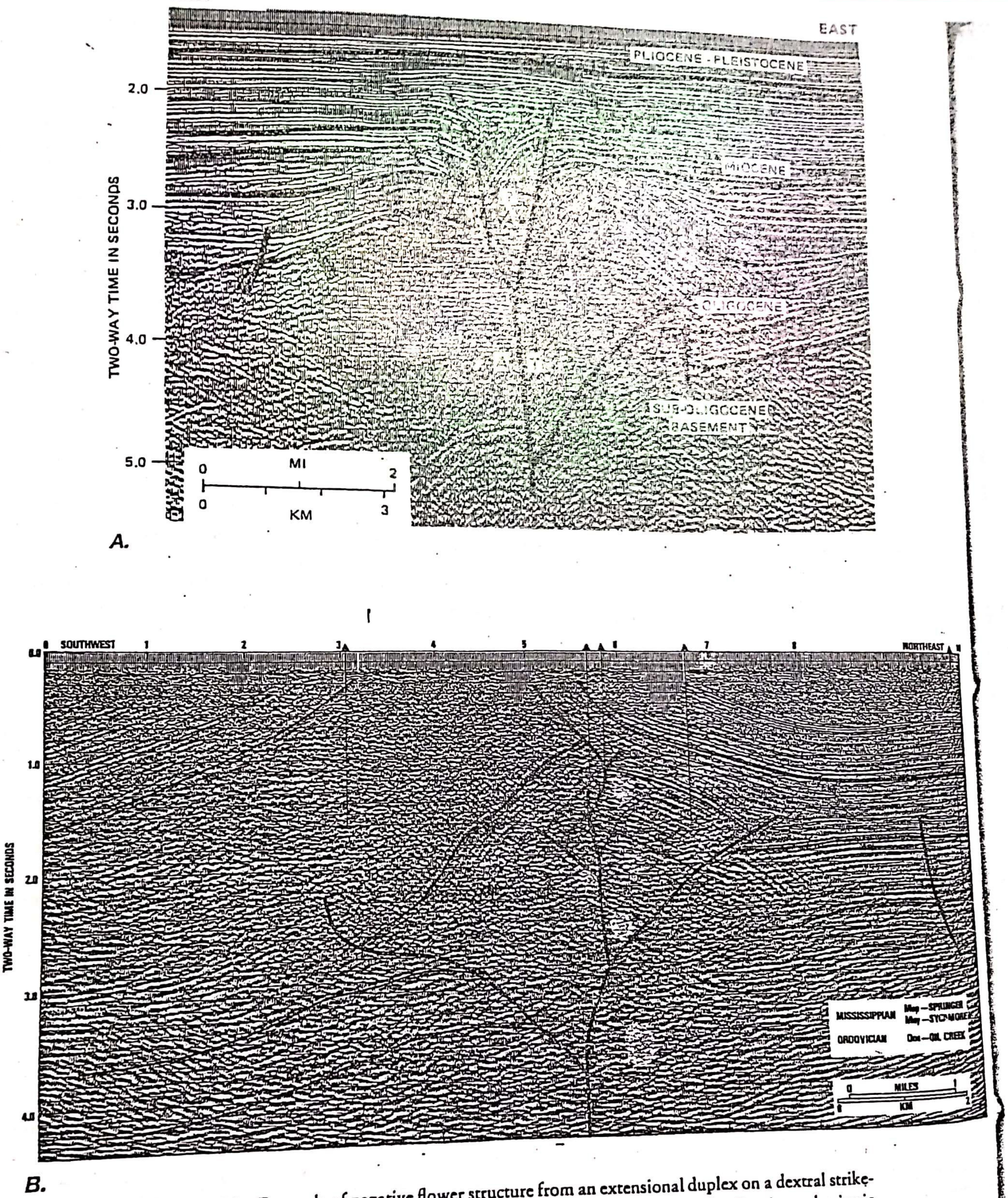

Figure 7.8*A*. Example of negative flower structure from an extensional duplex on a dextral strike-slip fault from the Andaman Sea between India and the Malay Peninsula. Unmigrated seismic reflection profile. *B*. Example of positive flower structure from a contractional duplex on a sinistral strike-slip fault in the Ardmore Basin, Oklahoma. Migrated seismic profile.

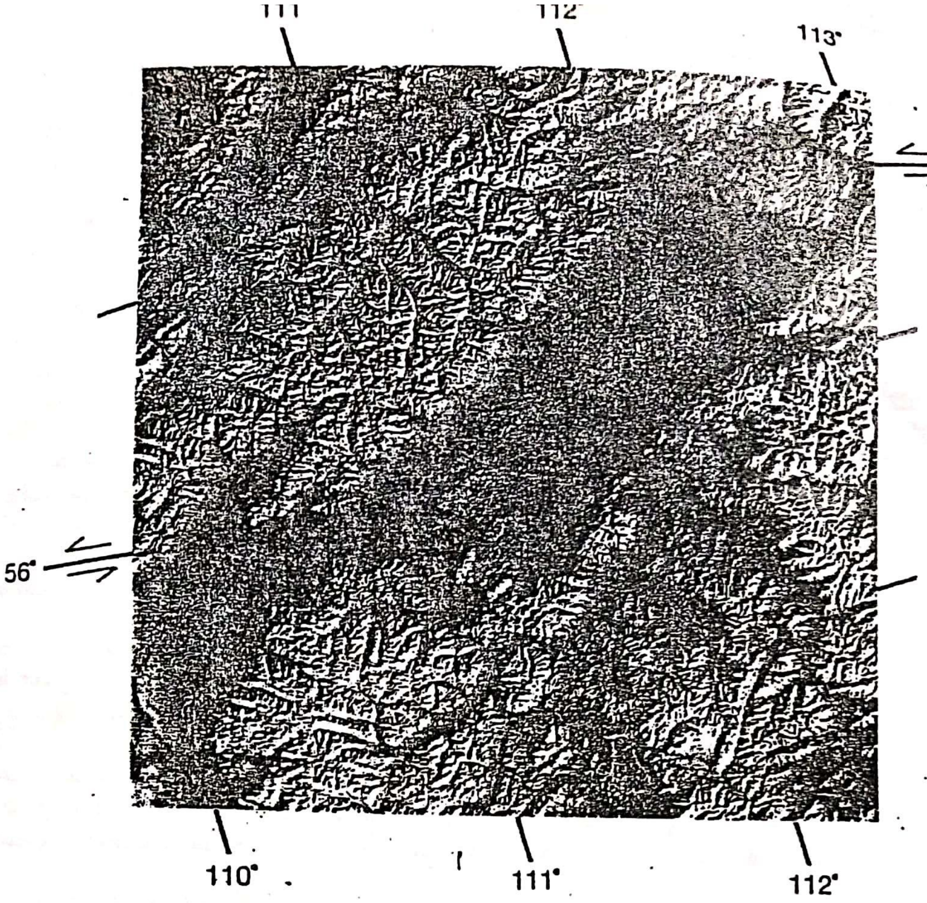

F
gra
apart
Lake B
(see loca
7.2B). The
at a left stepov
lateral strike-s
indicated at the
right and lower le
the photo. The basin
bounded by northeast-
trending normal fault
scarps.

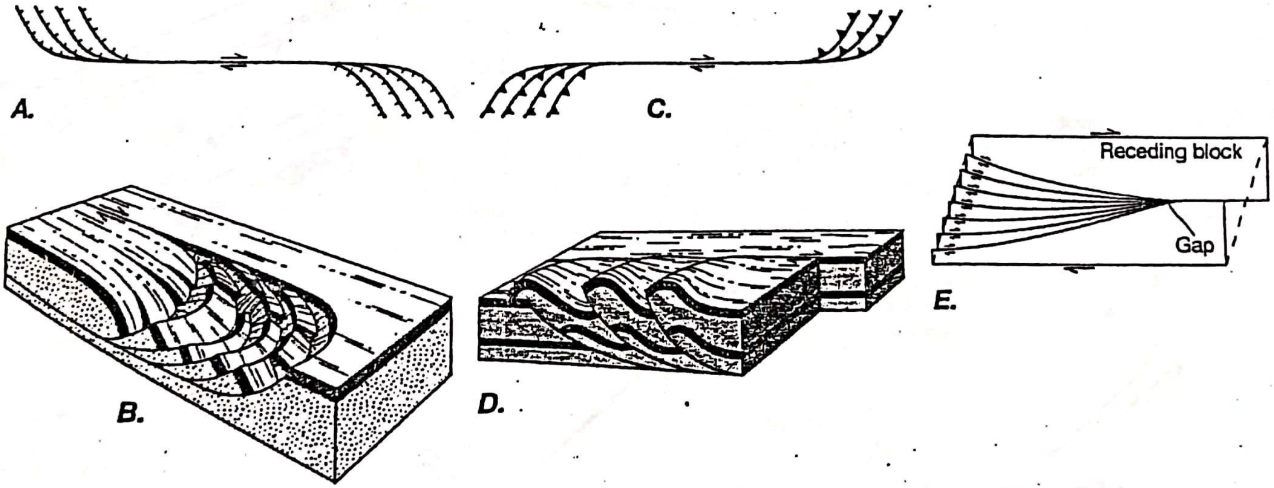

Figure 7.10 Termination of faults by the formation of imbricate fans. *A.* Geometry of extensional imbricate fans at the ends of a dextral fault. *B.* Extensional normal faulting at the termination of a dextral strike-slip fault. *C.* Geometry of contractional imbricate fans at the ends of a dextral fault. *D.* Contractional folding and thrust faulting at the termination of a dextral strike-slip fault. *E.* Geometry of a horsetail splay of strike-slip faults at the ends of a dextral strike-slip fault. The total displacement on the single fault at the right side of the block is the sum of small displacements on the individual splay faults at the left of the block. Splay faults tend to curve toward the receding block.

ommo-
n of crust at a spreading center
rust at a subduction zone.

uctural Associations of Strike-Slip Faults

Tear Faults

Strike-slip faults commonly are secondary structures associated with major faults and folds. Tear faults characteristically develop in regions of normal faulting (see Figures 5.11 and 5.12) and in fold and thrust sheets (see Section 6.2, Figures 6.7C, D and 6.13). They accommodate different amounts of extension or contraction in adjacent regions. The Jura Mountains of Switzerland (Figure 7.11; see Figure 6.20) are a classic example of a fold and thrust belt that is segmented by generally N-to-NW–trending tear faults. Fold hinges terminate laterally against the tear faults (compare Figure 6.13A, B), separating sections of the thrust sheet that have different magnitudes of displacement on the décollement.

Transcurrent and transform faults never occur as simple planar faults through the crust. They are characterized by complex zones of anastomosing, parallel, or *en echelon* faults that are not perfectly straight (Figure 7.2A) and that therefore result in a variety of accommodation structures (Figure 7.4).

An excellent example of an extensional duplex occurs on the active Dasht-E Bayaz fault in northeastern Iran (Figure 7.12). The duplex is in the process of developing at a left bend on the left-lateral fault. The main trace of the fault trends obliquely through the middle of the duplex. Subsidiary faults to the east and a dense concentration of fractures to the west outline two horses in which the fracture density is much lower. The inset on Figure 7.12 shows an idealization of the duplex geometry.

An even larger left bend in the San Andreas fault system occurs in Southern California in the region where the Garlock fault intersects the San Andreas (Figures 7.2A, 7.13). Here the contraction expected at a left bend in a dextral fault is reflected by the Transverse Ranges, a block of crust that has been uplifted on east-west–trending thrust faults (Figure 7.13). Along this contrac-

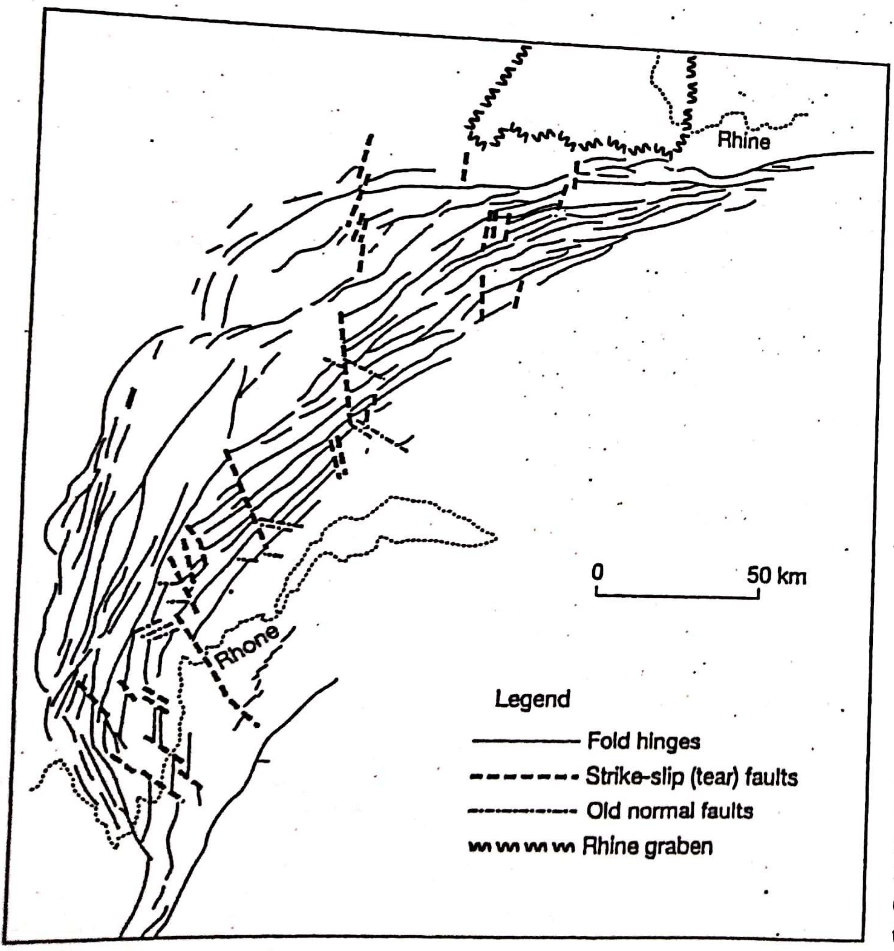

Figure 7.11 Tear faults in the Jura fold and thrust belt (see Figure 6.20 for location). The generalized map of Jura mountains shows the major fold axes tear faults, and the boundary of the Rhine graben. Note how fold axes tend to terminate against the tear faults.

Scanned by CamScanner

ıs simple
ıcterized
: en ech-
re 7.2A)
ıodation

plex oc-
heastern
s of de-
he main
: middle
a dense
o horses
he inset
: duplex

eas fault
n where
(Figures
left bend
Ranges,
st-west-
contrac-

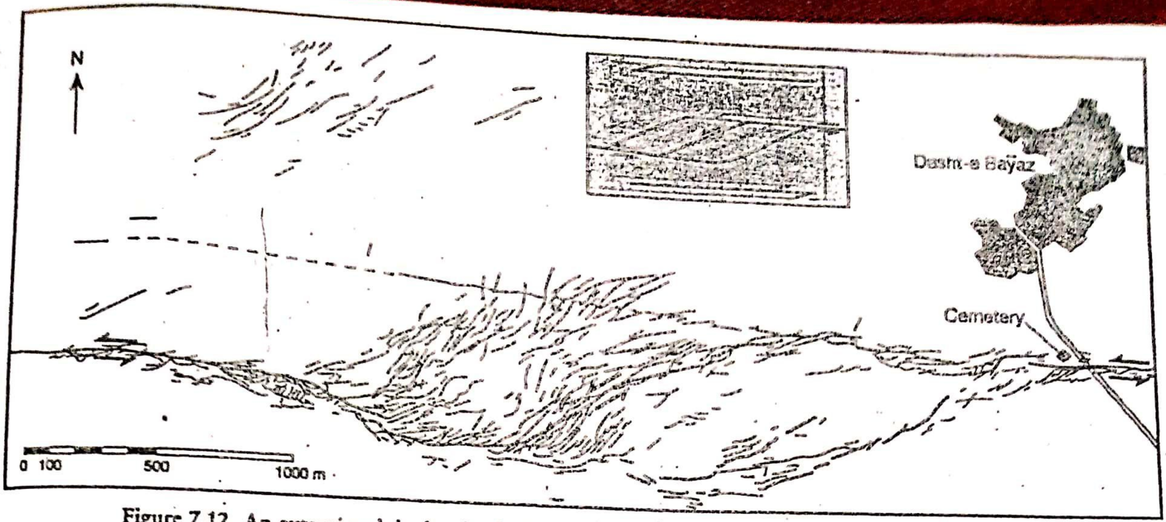

Figure 7.12 An extensional duplex developing on the active Dasht-e Bayaz fault in northeastern Iran.

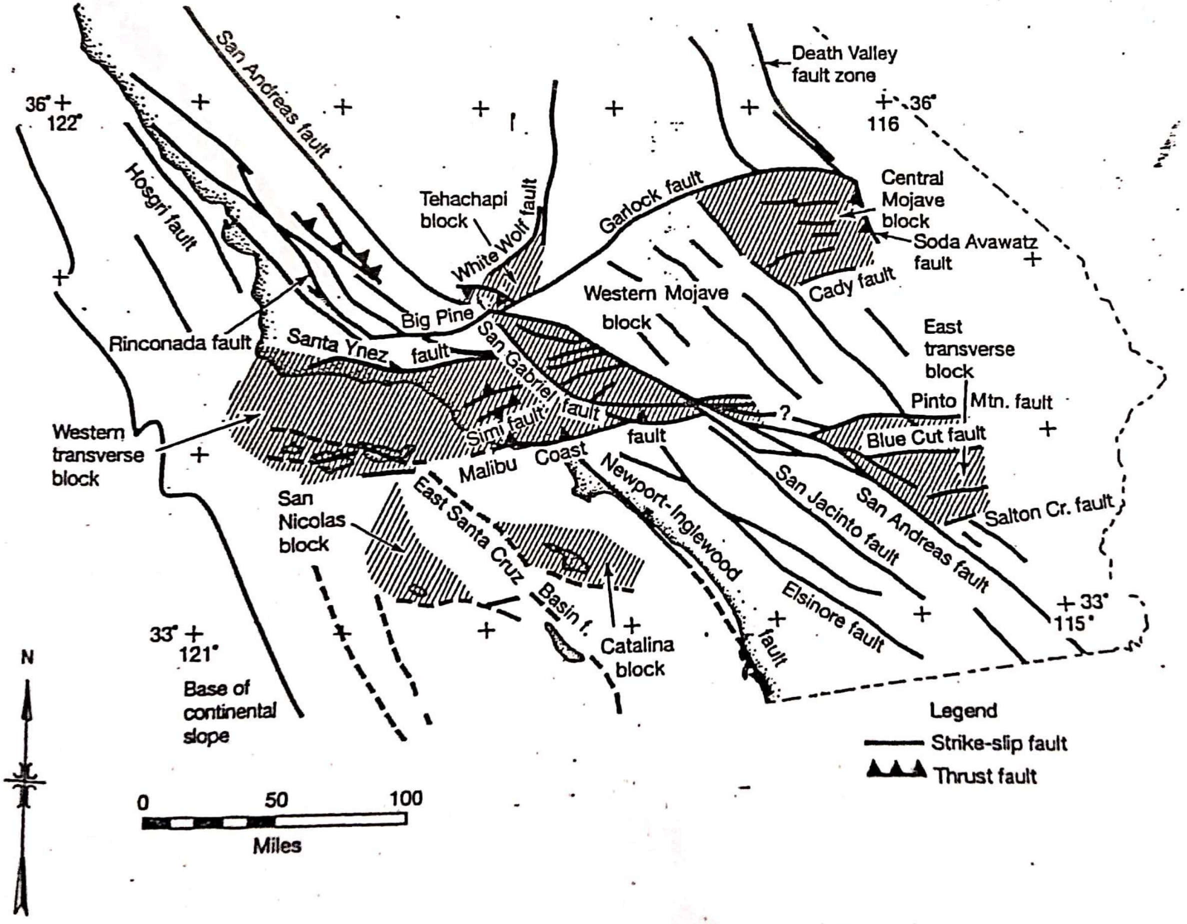

Figure 7.13 The San Andreas–Garlock fault systems in southern California.

fold and
ion). The
shows the
boundary
axes tend

tional bend, however, extensional basins are also present, illustrating the complex interplay of extensional and contractional structures in major strike-slip fault systems. These basins, which are filled with Neogene sediments, probably represent remnants of pull-apart basins that originally formed in extensional duplexes, some of which have been displaced from their original location.

The bend at the Transverse Ranges coincides with the intersection of the right-lateral San Andreas fault and the left-lateral Garlock and Big Pine faults. The Mojave block between the Garlock and San Andreas faults contains NW-trending dextral strike-slip faults as well as west-trending sinistral strike-slip faults, and parts of the block have experienced large amounts of roughly east–west extension. All these faults are no older than Tertiary. Understanding such a complex mosaic of faults requires an understanding of the history of each individual fault in relation to all the others—a challenge indeed! In the following section, we discuss one kinematic model for the faulting in this region that accounts for some aspects of the geology but is only a partial solution to the complex puzzle of deformation.

Terminations

Where strike-slip faults turn at their ends into thrust faults, the fault curves around, shallows in dip, and ends up trending approximately perpendicular to the direction of movement (Figure 7.10C, *D*). The active Quetta-Chaman fault system of Pakistan is a good example of this structure (Figure 7.14; see the west edge of Figure 7.2*B*). There the left-lateral Quetta-Chaman fault system terminates southward into a series of thrust faults and folds that in fact are part of a modern convergent plate margin.

At its east end, the Garlock fault apparently turns south and becomes a thrust fault that dips westward

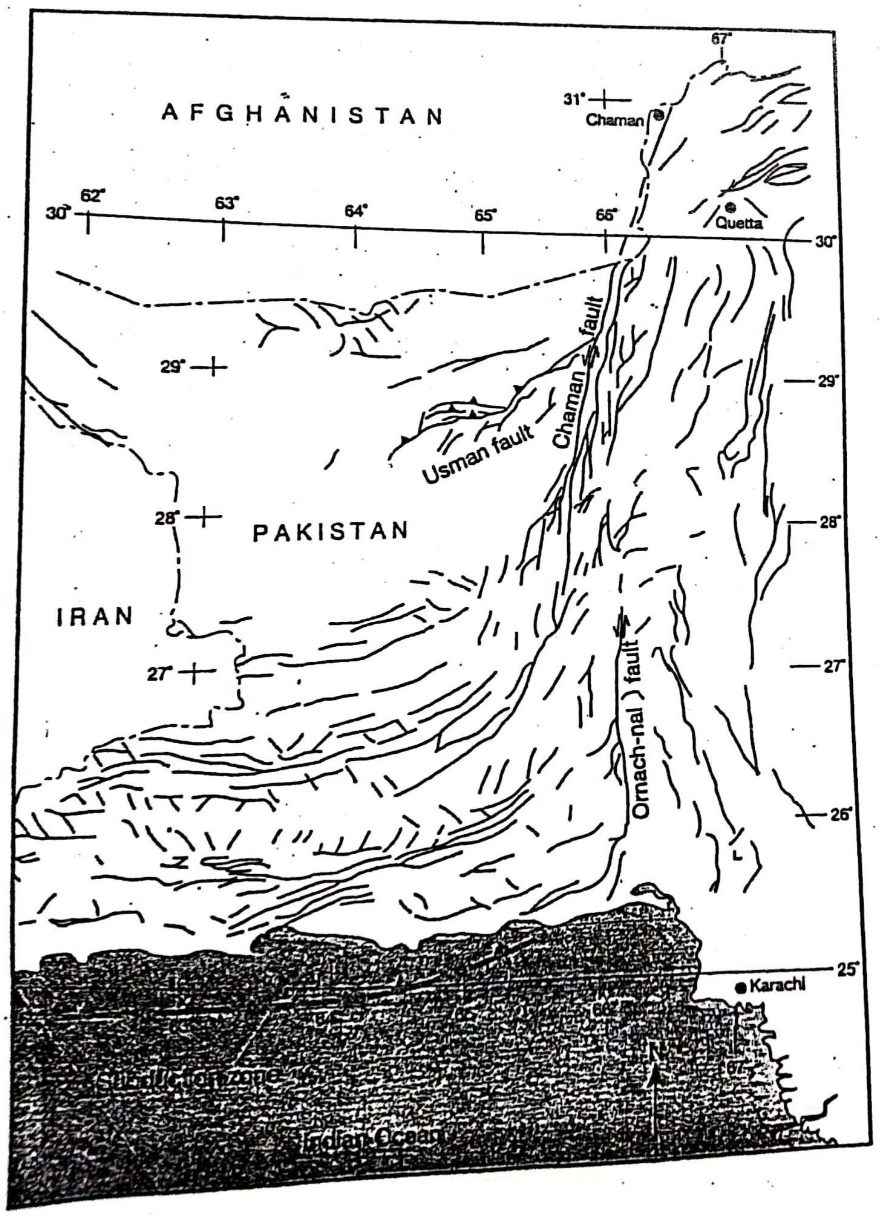

Figure 7.14 Map of faults in southern Pakistan. Major north-south-trending faults such as the Chaman and the Ornach-Nal faults are sinistral strike-slip faults that pass southward into an east-west-trending fold and thrust belt. Most of the east-west-trending faults are interpreted to be thrust faults synthetic to the subduction zone that lies in the Indian Ocean to the south. The short northeast- and northwest-trending faults in the south may be conjugate orientations of tear faults (see location in Figure 7.2*B*).

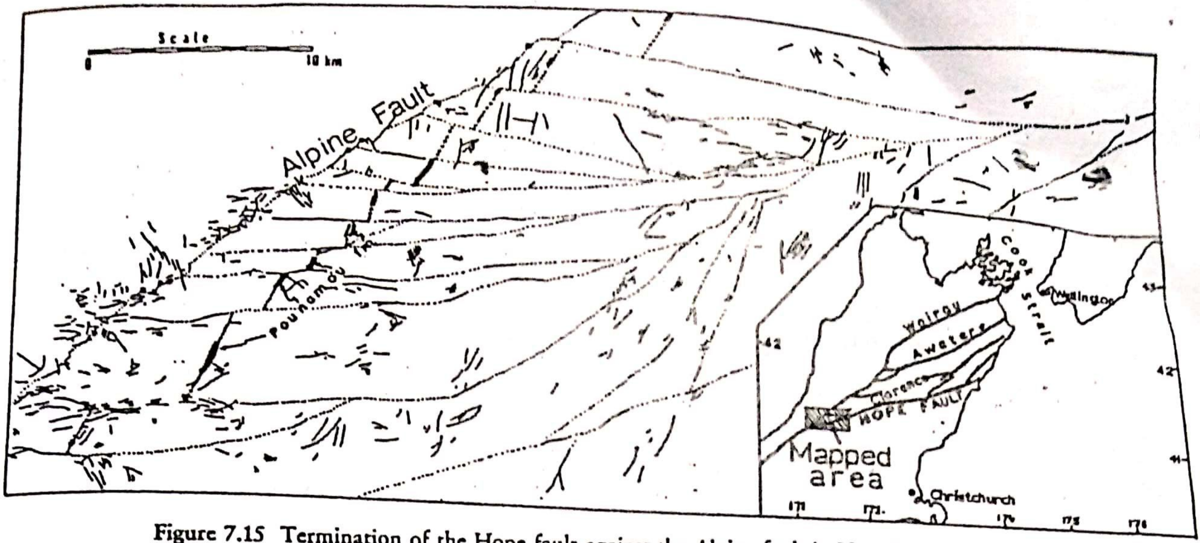

Figure 7.15 Termination of the Hope fault against the Alpine fault in New Zealand. Splaying of the Hope fault and curving of the splays toward the receding fault block are both evident. The displacement on the splays is defined by the offset of the Pounamou formation.

underneath the Soda and Avawatz Mountains (Figure 7.13). The geology here, however, is complicated by the intersection of the Garlock fault with the Death Valley fault zone.

The Hope fault, which is one strand of the Alpine fault system in New Zealand, provides a good example of the termination of a fault at a horsetail splay (Figure 7.15). The fault splays out against the Alpine fault with a relatively small amount of displacement distributed to each of the splays, as indicated by the horizontal separation of the Pounamou formation (compare Figure 7.10*E*).

7.4 Kinematic Models of Strike-Slip Fault Systems

As with other faults, it is useful to consider simplified kinematic models of strike-slip fault systems in order to gain insight into the complexities that can develop. In this section, we discuss models of distributed shear and of oblique strike-slip that can account for some of the folds, thrust faults, and normal faults that develop near strike-slip faults. We also discuss a model that accounts for some aspects of the regional deformation associated with the fault systems in southern California.

Many of the structures that develop near strike-slip faults can be accounted for by assuming that part of the shearing is distributed through the rock on either side of the fault. This model is illustrated in Figure 7.16, which shows two squares inscribed across a strike-slip fault (Figure 7.16*A*) that become separated by motion on the fault and also deformed into parallelograms by shearing distributed on either side of the fault (Figure 7.16*B*). As a result of the distributed shear, one diagonal of the square becomes shorter and the other longer. This model accounts for the formation and orientation of the folds and faults in Figure 7.4. The folds and thrust faults trend perpendicular to the direction of shortening and the normal faults trend perpendicular to the direction of lengthening.

The orientation of major strike-slip faults is not necessarily exactly parallel to the direction of relative

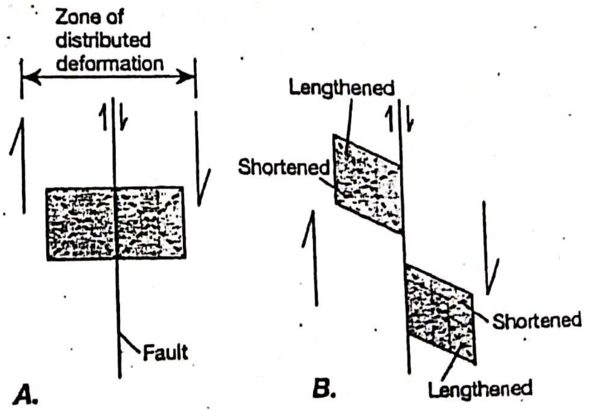

Figure 7.16 Kinematic model of a strike-slip fault where part of the shearing is distributed on either side of the fault. *A*. Before, and *B*. after shearing on and near the fault. Folds and thrust faults form at 45° to the main fault perpendicular to the direction of shortening, and normal faults form at 45° to the main fault perpendicular to the direction of lengthening (see Figure 7.4).

motion of the adjacent fault blocks. For [illegible] faults, for example, minor changes in plate motion can result in a component of contraction or extension across the fault that can be accommodated only by the development of other structures such as folds and thrust faults or normal faults, respectively. The contractional strike-slip model for the San Andreas fault may be the explanation for the uplift of the Coast Ranges on the west side of the Central Valley of California and for a series of thrust faults and folds that are currently active along the west side of the valley.

One kinematic model of the San Andreas system is shown in Figure 7.17. It represents an effort to integrate the numerous strike-slip faults in the region into a rational pattern. The model idealizes the domains of roughly parallel faults by assuming that they are perfectly straight faults defining the boundaries of rigid fault blocks (compare Figures 7.2*A* and 7.13). The domains comprise either a set of right-lateral NW-trending faults or a set of left-lateral faults originally trending N but now trending ENE. The model predicts that domains dominated by NW-trending right-lateral faults should not have rotated significantly during the deformation but that domains dominated by left-lateral faults, such as the Transverse Ranges, should have rotated clockwise by as much as 80° (Figure 7.17*B*). Subsequent to rotation, the Transverse Ranges have been split into eastern and western blocks by slip on the San Andreas fault. Slip on the fault system produces a net N–S shortening and E–W lengthening of southern California.

The assumption of rigid fault blocks requires that numerous gaps open during shearing, especially along domain boundaries (shaded areas in Figure 7.17*B*). Although deformation around these gaps would certainly be complex, many of the model gaps can be correlated with deep basins filled with large thicknesses of young, locally derived sediments. In addition, paleomagnetic determinations of the orientation of the paleopole in parts of the region are consistent with the large rotations, and with progressive rotation through time, as indicated by the model. These data are consistent with the model in that they permit only small counterclockwise rotation of the right-lateral fault domains, but large clockwise rotations of up to 70° to 80° for the western Transverse Ranges block.

Despite its complexity, this controversial model is not complete. It does not account, for example, for slip along the Garlock fault, for Basin and Range extension north of the Garlock, for extension in the Mojave block, for the rise of the Transverse Ranges on thrust faults associated with the contractional duplex along the San Andreas fault, or for any nonrigid behavior of the various fault blocks. Moreover, it does not consider the problem of the fault geometry and the displacement at depth. Nevertheless, such models are useful because they provide testable predictions and focus attention on critical problems.

As with other faults, complete models of strike-slip faults must account for the termination of the faults at depth as well as along strike (see Section 7.2). For large fault systems such as the San Andreas fault, the Alpine fault of New Zealand, and the Red River and Altyn Tagh faults in Asia, displacements of several hundred kilometers have accumulated. The only crustal

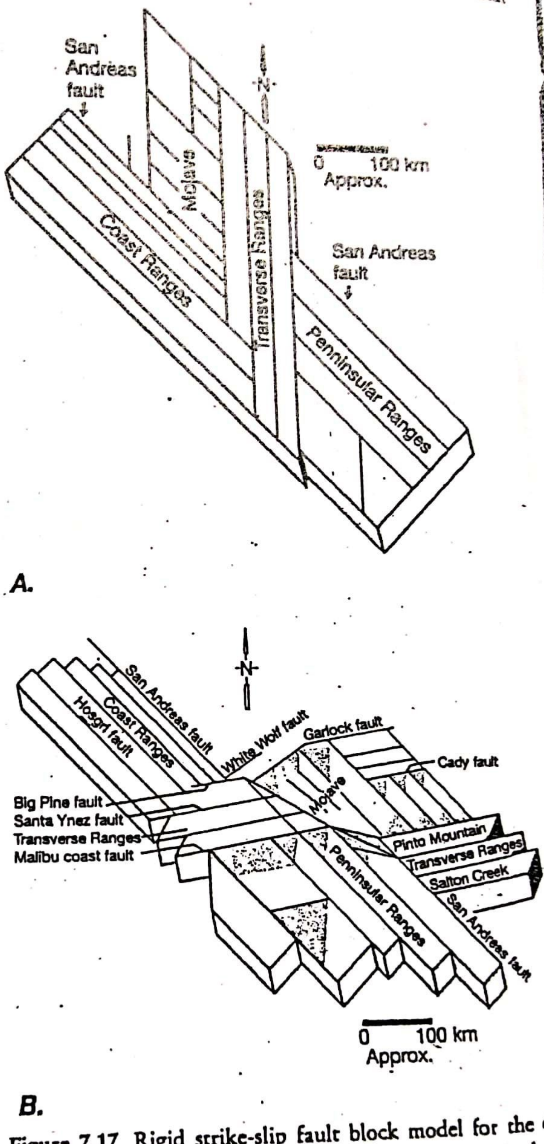

Figure 7.17 Rigid strike-slip fault block model for the development of the structures associated with the San Andreas fault system in southern California. *A.* Configuration of faults before displacement in Oligocene time. *B.* Present configuration, showing the right-lateral offset of the Transverse Ranges. Shaded areas indicate the location of basins that would open up as a result of sliding of the rigid blocks.

---

structures that se
mous displaceme

The functio
form fault betwe
ifornia and off t
Oregon is well r
gashears in Asia
proposed, but ex
structures thems
and their associa
the collision zo
such large displ
quire involveme
rocks.

7.5 Analy
Strike

In Section 4.3 v
of determining
matching of c
sides of the fa
nations. For re
of distinguishi
is an importa
however, that
hundred kilon
a fault other
an example c
on the San A

The gec
in Figure 7.
planar, norr
imagine Fig
faults instea
the angle of
ary, ϕ is th
boundary,
$w = L \sin$ (
basic paran

Aydin, A.,
and th
Christie-Bl
basin
and N
forma
tolog
Garfunkel

structures that seem capable of absorbing such enormous displacements are plate boundaries.

The function of the San Andreas fault as a transform fault between triple junctions in the Gulf of California and off the northwest coast of California and Oregon is well recognized. The association of the megashears in Asia with the collision of India has been proposed, but except for the Quetta-Chaman faults, the structures themselves do not serve as transform faults, and their association with plate boundaries other than the collision zone is not obvious. Accommodation of such large displacements, however, would seem to require involvement not just of crustal, but also of mantle, rocks.

7.5 Analysis of Displacement on Strike-Slip Faults

In Section 4.3 we discussed the most important methods of determining displacement on strike-slip faults. The matching of displaced geologic features on opposite sides of the fault provides the most reliable determinations. For relatively small displacements, the problem of distinguishing the separation from the displacement is an important one. The possibility is rather remote, however, that horizontal separations on the order of a hundred kilometers were produced by displacement on a fault other than a strike-slip fault. Figure 4.18 shows an example of the determination of large displacement on the San Andreas fault.

The geometric model used for strike-slip faulting in Figure 7.17 is identical to the model for rotating planar, normal faults (Figure 5.22B). One need only imagine Figure 5.22B to be a map view of strike-slip faults instead of a cross section of normal faults: θ is the angle of rotation of the blocks from the fixed boundary, ϕ is the angle between the faults and the fixed boundary, and the width of the fault block is $w = L \sin(\phi + \theta)$. Because $L \sin\theta = d \sin\phi$, the four basic parameters describing the deformation—d, w, ϕ, and θ—are related by the equation

$$\frac{d}{w} = \left(\frac{d}{L}\right)\left(\frac{L}{w}\right) = \left[\frac{\sin\theta}{\sin\phi}\right]\left[\frac{1}{\sin(\theta + \phi)}\right]$$

which must be satisfied if the model is correct. In principle, all the parameters are measurable. We can determine the rotation θ of a crustal block by measuring the rotation of the paleomagnetic pole; we can measure the present angle ϕ of the faults from a fixed boundary, we can find the width w of a particular fault block, and we can use the displacement of geologic features on individual faults to determine the displacement d. As discussed in Section 7.4, application of this test of the model to the southern California region has confirmed the predictions of the model.

7.6 Balancing Strike-Slip Faults

In Section 4.5 we discuss the technique of balancing cross sections of dip-slip (normal and thrust) faults. The assumptions used in balancing are valid only when the deformation has been essentially two-dimensional such that no net movement of material has taken place into or out of the plane of the cross section. Vertical cross sections perpendicular to strike-slip faults do not meet this requirement, and it is generally inappropriate to attempt to balance such cross sections.

The appropriate plane for possible balancing of strike-slip faults is the plane of the map, which contains the fault slip vector. This plane is generally parallel to bedding, however, so the boundaries that are used to measure lengths and areas in balancing dip-slip faults are commonly not available for strike-slip faults. Moreover, the vertical displacement that accompanies deformation at bends and stepovers violates the strict condition of two-dimensional deformation. Thus any valid balancing of strike-slip faults would have to account for the motion normal to the plane of balancing.

Because of these difficulties, the use of balanced sections as a method of analyzing strike-slip fault zones is not commonplace.

Additional Readings

Aydin, A., and A. Nur. 1982. Evolution of pull-apart basins and their scale independence. *Tectonics* 1: 91–105.

Christie-Blick, N. and K. T. Biddle. 1985. Deformation and basin formation along strike-slip faults. In K. T. Biddle and N. Christie-Blick (ed.), Strike-slip deformation, basin formation, and sedimentation. *Society of economic pleontologists and mineralogists special publication 37*, 1–34.

Garfunkel, Z. and H. Ron. 1985. Block rotation and deformation by strike-slip faults 2: The properties of a type of macroscopic discontinuous deformation. *J. Geophys. Research* 90: 8589–8602.

Sylvester, A. G. 1988. Strike-slip faults. *Geol. Soc. Am. Bull.* 100: 1666–1703.

Woodcock, N. J., and M. Fischer. 1986. Strike-slip duplexes. *J. Struct. Geol.* 8: 725–35.